Discrete $\{Gd^{III}_4M\}$ (M=Gd^{III} or Co^{II}) pentanuclear complexes: A new class of metal-organophosphate molecular coolers

Sandeep K. Gupta,[a] Aijaz A. Dar,[a] Thayalan Rajeshkumar, [a] Subramaniam Kuppuswamy, [a] Stuart K. Langley,[b] Keith S. Murray,[b] Gopalan Rajaraman[a] and Ramaswamy Murugavel[a]

[a]*Department of Chemistry, Indian Institute of Technology Bombay, Powai, Mumbai, Maharashtra, India-400076*
[c]*School of Chemistry, Monash University, Clayton, Victoria 3800, Australia*

Experimental Section:
All reactions were carried out under ambient conditions without any special precautions. All the starting materials and the products were found to be stable towards moisture and air. The melting points were measured in glass capillaries. Infrared spectra were recorded on a Perkin-Elmer Spectrum One FT-IR spectrometer as KBr diluted discs. Microanalyses were performed on a Thermo Finnigan (FLASH EA 1112) microanalyzer. Thermo gravimetric analyses were carried out with a Perkin-Elmer thermal analysis system at the heating rate of 10 °C/min under a stream of dry nitrogen gas. Solvents were pre-distilled before use. Gadolinium(III) nitrate hydrate, 99.9%(Alfa Aesar), Cobalt(II) acetate tetrahydrate (Spectrochem), N,N,N,N-Tetramethylethylene diamine/(tmeda) (Spectrochem) , 2,6-di-iso-propylphenol (Sigma Aldrich) were used as received. The 2,6-di-iso-propylphenylphosphate(dippH_2) was synthesized according to the reported method.[1] $[Co(dipp)(DMSO)]_4$ was synthesized from cobalt(II) acetate tetrahydrate and dippH_2 in DMSO by following similar synthetic protocol reported earlier for the preparation of the zinc analogue.[2]

$[Gd_5(\mu_3\text{-}OH)(NO_3)_2(dipp)_6(CH_3OH)_7(H_2O)_4].5CH_3OH$ (1): To a solution of $Gd(NO_3)_3.xH_2O$ (0.045 g, 0.10 mmol) in methanol (10 mL) was added a solution of dippH_2(0.026 g, 0.10 mmol) in methanol (10 mL). The solution was stirred well and tmeda (0.023mg, 0.20 mmol) was added to it. The reaction mixture was heated at 70°C for 3h and was then cooled to room temperature. The solution was filtered and the clear filtrate was kept for crystallization at room temperature. Crystals from the mother liquor were obtained within a period of two weeks. Yield: 0.038 g (78%, based on dippH_2). M.p: >250°C. Anal. Calcd for $C_{84}H_{159}Gd_5N_2O_{47}P_6$: C, 34.54; H, 5.49; N, 0.96. Found: C, 34.76; H, 5.57; N, 1.04. FT-IR (KBr, cm^{-1}): 3565(br), 3400(br), 2966(s), 2930(m), 2870(w), 1622(br), 1466(s), 1440(s), 1384(vs), 1362(m), 1335(s), 1256(s), 1187(s), 1148(vs), 1047(s), 1011(vs), 916(vs), 882(w), 770(s), 750(w), 663(w), 600(w), 546(s), 523(s). TGA: Temp. range °C (% Weight loss): 30-123 (5.2); 123-179 (3.5); 179-275 (9.9); 275-800 (29.2); 800-1000 (2.7).

$[Gd_4Co_1(\mu_3\text{-}O)(dipp)_6(DMSO)_6(MeOH)_2].H_2O$ (2): A solution of $Gd(NO_3)_3.xH_2O$ (0.090 g, 0.20 mmol) in methanol (10 mL) was added to the solution of $[Co(dipp)(DMSO)]_4$ (0.079 g, 0.05 mmol) in DMSO (5 mL). The resultant solution was stirred well at room temperature for 15-20 minutes to yield light pink solution. The solution was filtered and CH_2Cl_2 (5 mL) was layered over it and and kept for crystallization at room temperature to yield the product as blue crystalline materials after the period of 2 weeks. Yield: 0.075 g (55% based on $[Co(dipp)(DMSO)]_4$). Mp: > 250 °C. Anal. Calcd for $C_{86}H_{148}Co_1Gd_4O_{34}P_6S_6$: C, 36.99; H, 5.34; S, 6.89. Found: C, 36.52; H, 5.29; S, 6.57. FT-IT (KBr, cm^{-1}): 3551(br), 3409(br), 2964(s),

2930(s), 2927(m), 2868(w), 1618(br), 1466(s), 1439(s), 1384(vs), 1361(m), 1336(m), 1256(s), 1188(s), 1152(vs), 1046(s), 1008(vs), 920(s), 882(w), 771(s), 749(w), 543(s), 519(m). Temp. range ^{o}C (% Weight loss): 30-200(2.5); 200-700 (48.3); 700-1000 (6.8).

Mechanism for the formation of pentanuclear cluster

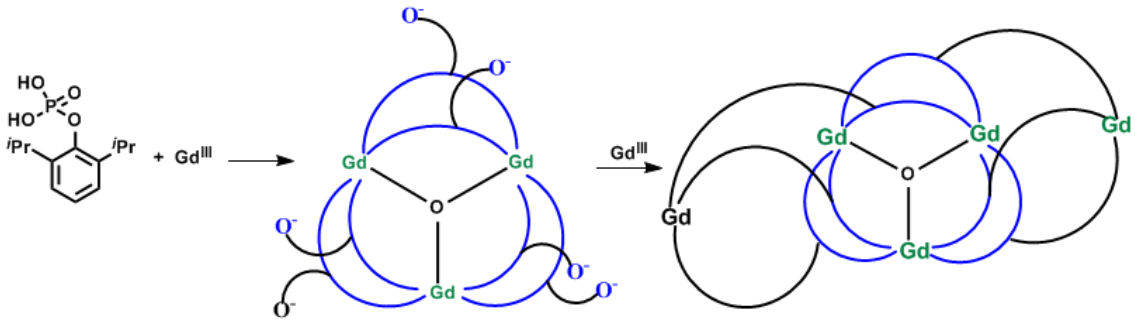

Figure S1. Formation of the pentanuclear cluster using the dangling oxygen atoms of the phosphate ligand from the trinuclear oxo/hydroxo metal cluster

Fourier Transform Infrared Spectroscopy and Thermal Analysis:

The absence of any broad absorption band around 2300 cm^{-1} region in the FT-IR spectra of **1** and **2** (Supporting information, Figure S2 and S3) supports the complete deprotonation of the phosphate ligand. The strong absorption bands at 1148, 1047 and 1011 cm^{-1} for **1** and 1152, 1046 and 1008 cm^{-1} for **2** correspond to the P=O stretching vibrations and M−O−P asymmetric and symmetric stretching vibrations, respectively. The TGA profile for **1** shows gradual weight loss due to the loss of lattice and coordinated solvents molecules from 50^{o}C and sharp weight loss from 300 ^{o}C due to the decomposition of metal phosphate core whereas compound **2** shows minimal weight loss upto 200 ^{o}C followed by sharp weight loss due to the decomposition of the core (Supporting information, Figure S4).

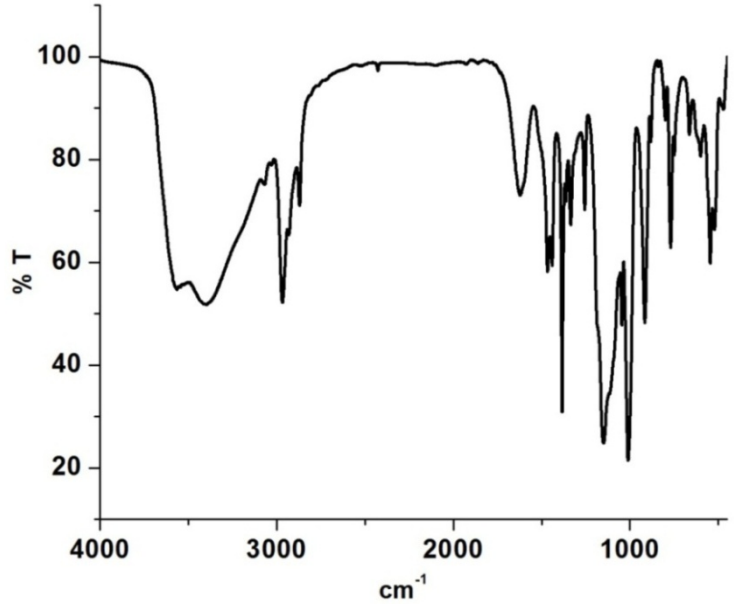

Figure S2. FT-IR spectrum of compound **1** as diluted KBr disc.

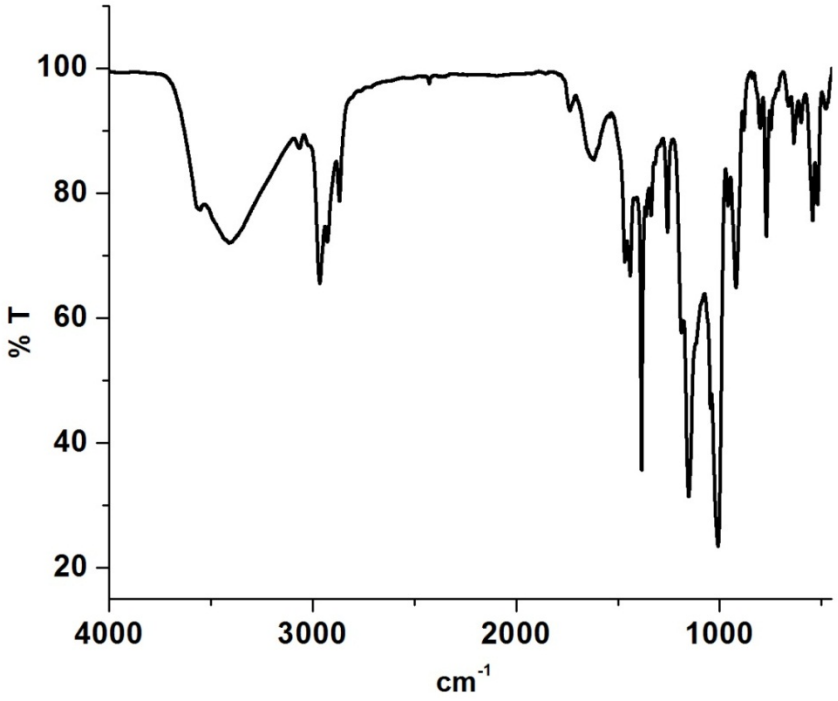

Figure S3. FT-IR spectrum of compound **2** as diluted KBr disc.

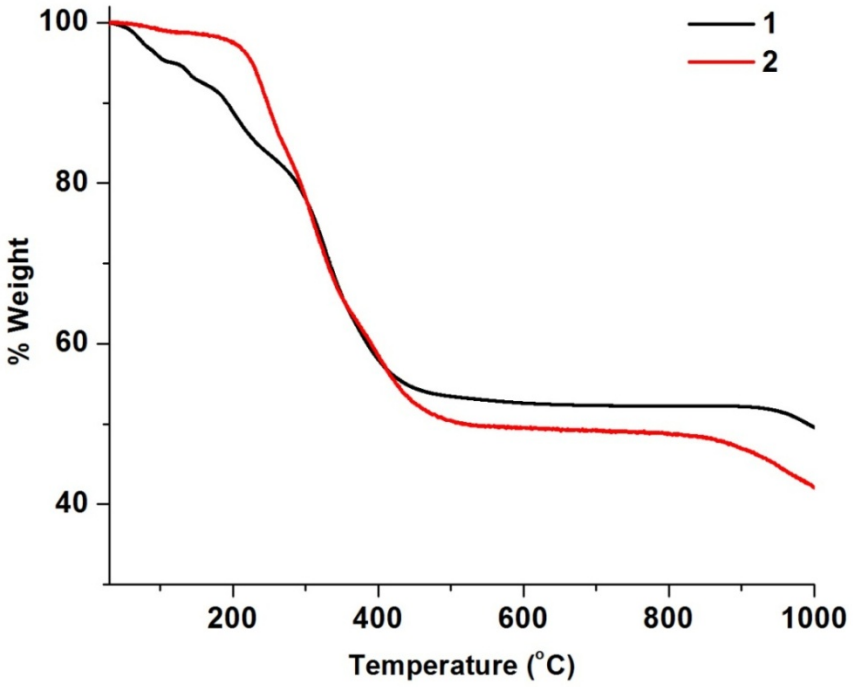

Figure S4. TGA profile for compound **1** and **2**.

X-ray Structure Analysis: Intensity data for compound **1** and **2** was collected on a Rigaku Saturn724+ diffractometer. All calculations were carried out using the programs in WinGX module.[3] The structure was solved in each case by direct methods (SIR-92).[4] The final refinement of the structure was carried out using full least-squares methods on F2 using SHELXL-2012.[5] Crystals were mounted on a micro-loop using paraffin oil and the intensity data were collected at 150K. Some H atoms couldn't be located and refined but has been included in the molecular formula**.** In spite of repeated crystallization, complex **2** yielded only poor quality data. This is due to extremely small size of crystals (0.04 x 0.08 x 0.15) which lose solvent molecules and crumble as they were fished out of the mother liquor for mounting.

Table S1. Crystal Data and Structure Refinement Details for Compounds **1** and **2**.

Compound	**1**	**2**
Identification code	SKG423	AJZ611
Empirical formula	$C_{84}H_{159}Gd_5N_2O_{47}P_6$	$C_{86}H_{148}Co_1Gd_4O_{34}P_6S_6$
Fw	2921.24	2792.24
Temp, [K]	123(2)	123(2)
Crystal system	Triclinic	Monoclinic
Space group	P-*1*	P 21/n
a, [Å]	14.110(3)	15.558(4)
b, [Å]	16.918(3)	51.036(13)
c, [Å]	25.380(4)	16.038(5)
α, [°]	99.378(3)	90
β, [°]	90.744(4)	111.128(4)°
γ, [°]	105.488(3)	90
V, [Å^3]	5750.3(18)	11878(6)
Z	2	4
D(calcd), [g/cm^3]	1.686	1.560
μ [mm^{-1}]	3.014	2.600
Crystal size	0.12 x 0.15 x 0.25	0.04 x 0.08 x 0.15
θ range, [deg]	2.249 to 25.500	2.315 to 25.100
Reflections collected	45450	81078
Independent reflections	21147 [R(int) = 0.0441]	20996 [R(int) = 0.1412]
GOF	1.145	1.288
R1(I_0>2σ(I_0))	0.0552	0.1448
wR2 (all data)	0.1302	0.2713
largest hole and peak [e · Å^{-3}]	2.482 and -2.135	2.198 and -1.616

Table S2. Selected bond lengths [Å] and angles [°] for compound **1**.

Gd(1)-O(18)	2.262(5)
Gd(1)-O(21)	2.302(5)
Gd(1)-O(5)	2.332(5)
Gd(1)-O(3)	2.379(5)
Gd(1)-O(25)	2.398(5)
Gd(1)-O(33)	2.481(6)
Gd(1)-O(32)	2.520(5)
Gd(1)-O(2)	2.544(5)
Gd(1)-Gd(2)	3.8865(8)
Gd(1)-Gd(3)	3.9399(9)
Gd(2)-O(13)	2.241(5)
Gd(2)-O(22)	2.271(5)
Gd(2)-O(2)	2.329(5)
Gd(2)-O(25)	2.375(5)
Gd(2)-O(10)	2.400(5)
Gd(2)-O(34)	2.410(5)
Gd(2)-O(9)	2.514(5)
Gd(2)-Gd(3)	3.9192(8)
Gd(3)-O(14)	2.274(5)
Gd(3)-O(17)	2.317(5)
Gd(3)-O(9)	2.387(5)
Gd(3)-O(35)	2.422(5)
Gd(3)-O(6)	2.445(5)
Gd(3)-O(25)	2.448(5)
Gd(3)-O(36)	2.528(5)
Gd(3)-O(5)	2.535(5)
Gd(4)-O(15)	2.270(5)
Gd(4)-O(23)	2.276(5)
Gd(4)-O(19)	2.288(5)
Gd(4)-O(39)	2.449(5)
Gd(4)-O(37)	2.452(6)
Gd(4)-O(27)	2.457(5)
Gd(4)-O(38)	2.460(5)
Gd(4)-O(26)	2.642(6)
Gd(5)-O(11)	2.243(5)
Gd(5)-O(7)	2.284(5)
Gd(5)-O(1)	2.308(5)
Gd(5)-O(41)	2.391(5)
Gd(5)-O(42)	2.414(6)
Gd(5)-O(29)	2.520(8)

Gd(5)-O(40)	2.563(9)
Gd(5)-O(30)	2.605(7)
P(1)-O(1)	1.504(6)
P(1)-O(3)	1.519(5)
P(1)-O(2)	1.522(5)
P(1)-O(4)	1.593(5)
P(2)-O(7)	1.500(5)
P(2)-O(6)	1.522(5)
P(2)-O(5)	1.523(5)
P(2)-O(8)	1.623(5)
P(3)-O(11)	1.507(5)
P(3)-O(10)	1.513(6)
P(3)-O(9)	1.524(5)
P(3)-O(12)	1.617(5)
P(4)-O(14)	1.505(5)
P(4)-O(15)	1.513(5)
P(4)-O(13)	1.518(5)
P(4)-O(16)	1.620(5)
P(5)-O(17)	1.509(5)
P(5)-O(19)	1.512(5)
P(5)-O(18)	1.521(5)
P(5)-O(20)	1.626(5)
P(6)-O(23)	1.504(5)
P(6)-O(22)	1.513(5)
P(6)-O(21)	1.517(5)
P(6)-O(24)	1.638(5)
O(4)-C(1)	1.408(9)
O(8)-C(13)	1.414(10)
O(12)-C(25)	1.411(12)
O(16)-C(37)	1.397(8)
O(20)-C(49)	1.393(8)
O(24)-C(61)	1.398(9)
O(25)-H(25)	0.74(8)
O(18)-Gd(1)-O(21)	92.83(18)
O(18)-Gd(1)-O(5)	88.69(18)
O(21)-Gd(1)-O(5)	151.09(17)
O(18)-Gd(1)-O(3)	150.32(18)
O(21)-Gd(1)-O(3)	105.43(18)
O(5)-Gd(1)-O(3)	86.32(18)
O(18)-Gd(1)-O(25)	80.68(17)

O(21)-Gd(1)-O(25)	79.79(17)
O(5)-Gd(1)-O(25)	71.97(17)
O(3)-Gd(1)-O(25)	124.95(17)
O(18)-Gd(1)-O(33)	86.6(2)
O(21)-Gd(1)-O(33)	65.7(2)
O(5)-Gd(1)-O(33)	143.2(2)
O(3)-Gd(1)-O(33)	80.2(2)
O(25)-Gd(1)-O(33)	142.5(2)
O(18)-Gd(1)-O(32)	74.28(19)
O(21)-Gd(1)-O(32)	135.28(18)
O(5)-Gd(1)-O(32)	72.72(18)
O(3)-Gd(1)-O(32)	76.29(19)
O(25)-Gd(1)-O(32)	136.73(18)
O(33)-Gd(1)-O(32)	70.9(2)
O(18)-Gd(1)-O(2)	149.80(16)
O(21)-Gd(1)-O(2)	79.64(17)
O(5)-Gd(1)-O(2)	84.62(17)
O(3)-Gd(1)-O(2)	58.58(16)
O(25)-Gd(1)-O(2)	69.24(16)
O(33)-Gd(1)-O(2)	115.7(2)
O(32)-Gd(1)-O(2)	130.60(19)
O(13)-Gd(2)-O(22)	93.90(18)
O(13)-Gd(2)-O(2)	154.39(17)
O(22)-Gd(2)-O(2)	85.53(18)
O(13)-Gd(2)-O(25)	81.16(17)
O(22)-Gd(2)-O(25)	82.81(17)
O(2)-Gd(2)-O(25)	73.36(17)
O(13)-Gd(2)-O(10)	105.21(18)
O(22)-Gd(2)-O(10)	145.50(18)
O(2)-Gd(2)-O(10)	88.83(18)
O(25)-Gd(2)-O(10)	127.81(17)
O(13)-Gd(2)-O(34)	86.67(19)
O(22)-Gd(2)-O(34)	78.56(18)
O(2)-Gd(2)-O(34)	118.1(2)
O(25)-Gd(2)-O(34)	156.96(19)
O(10)-Gd(2)-O(34)	74.28(19)
O(13)-Gd(2)-O(9)	87.89(17)
O(22)-Gd(2)-O(9)	151.25(16)
O(2)-Gd(2)-O(9)	80.82(17)
O(25)-Gd(2)-O(9)	69.10(16)
O(10)-Gd(2)-O(9)	59.67(16)

O(34)-Gd(2)-O(9)	130.18(17)
O(14)-Gd(3)-O(17)	91.52(18)
O(14)-Gd(3)-O(9)	89.17(17)
O(17)-Gd(3)-O(9)	145.25(17)
O(14)-Gd(3)-O(35)	84.61(19)
O(17)-Gd(3)-O(35)	73.49(17)
O(9)-Gd(3)-O(35)	141.04(17)
O(14)-Gd(3)-O(6)	151.49(17)
O(17)-Gd(3)-O(6)	111.13(17)
O(9)-Gd(3)-O(6)	81.89(17)
O(35)-Gd(3)-O(6)	85.54(18)
O(14)-Gd(3)-O(25)	78.08(17)
O(17)-Gd(3)-O(25)	76.14(17)
O(9)-Gd(3)-O(25)	70.04(16)
O(35)-Gd(3)-O(25)	144.42(18)
O(6)-Gd(3)-O(25)	122.98(16)
O(14)-Gd(3)-O(36)	77.64(19)
O(17)-Gd(3)-O(36)	143.01(18)
O(9)-Gd(3)-O(36)	70.72(17)
O(35)-Gd(3)-O(36)	70.37(18)
O(6)-Gd(3)-O(36)	73.85(18)
O(25)-Gd(3)-O(36)	133.64(18)
O(14)-Gd(3)-O(5)	145.83(17)
O(17)-Gd(3)-O(5)	82.10(16)
O(9)-Gd(3)-O(5)	78.09(16)
O(35)-Gd(3)-O(5)	124.66(18)
O(6)-Gd(3)-O(5)	58.22(16)
O(25)-Gd(3)-O(5)	67.79(16)
O(36)-Gd(3)-O(5)	125.59(17)
O(15)-Gd(4)-O(23)	89.30(18)
O(15)-Gd(4)-O(19)	83.51(18)
O(23)-Gd(4)-O(19)	88.38(18)
O(15)-Gd(4)-O(39)	152.01(19)
O(23)-Gd(4)-O(39)	98.0(2)
O(19)-Gd(4)-O(39)	69.79(18)
O(15)-Gd(4)-O(37)	69.79(18)
O(23)-Gd(4)-O(37)	95.6(2)
O(19)-Gd(4)-O(37)	152.91(18)
O(39)-Gd(4)-O(37)	135.5(2)
O(15)-Gd(4)-O(27)	82.66(19)
O(23)-Gd(4)-O(27)	171.00(18)

O(19)-Gd(4)-O(27)	86.69(19)
O(39)-Gd(4)-O(27)	87.4(2)
O(37)-Gd(4)-O(27)	85.5(2)
O(15)-Gd(4)-O(38)	135.36(18)
O(23)-Gd(4)-O(38)	71.83(17)
O(19)-Gd(4)-O(38)	133.86(18)
O(39)-Gd(4)-O(38)	72.24(19)
O(37)-Gd(4)-O(38)	72.24(18)
O(27)-Gd(4)-O(38)	116.87(18)
O(15)-Gd(4)-O(26)	118.66(18)
O(23)-Gd(4)-O(26)	138.87(17)
O(19)-Gd(4)-O(26)	122.06(18)
O(39)-Gd(4)-O(26)	71.9(2)
O(37)-Gd(4)-O(26)	70.2(2)
O(27)-Gd(4)-O(26)	49.77(18)
O(38)-Gd(4)-O(26)	67.10(17)
O(11)-Gd(5)-O(7)	84.32(18)
O(11)-Gd(5)-O(1)	89.05(19)
O(7)-Gd(5)-O(1)	84.81(19)
O(11)-Gd(5)-O(41)	90.2(2)
O(7)-Gd(5)-O(41)	79.29(19)
O(1)-Gd(5)-O(41)	164.08(19)
O(11)-Gd(5)-O(42)	161.0(2)
O(7)-Gd(5)-O(42)	77.3(2)

O(1)-Gd(5)-O(42)	84.5(2)
O(41)-Gd(5)-O(42)	91.2(2)
O(11)-Gd(5)-O(29)	72.8(2)
O(7)-Gd(5)-O(29)	146.0(3)
O(1)-Gd(5)-O(29)	118.7(2)
O(41)-Gd(5)-O(29)	76.1(3)
O(42)-Gd(5)-O(29)	125.9(2)
O(11)-Gd(5)-O(40)	106.1(3)
O(7)-Gd(5)-O(40)	143.9(3)
O(1)-Gd(5)-O(40)	61.5(2)
O(41)-Gd(5)-O(40)	133.7(3)
O(42)-Gd(5)-O(40)	86.5(3)
O(29)-Gd(5)-O(40)	68.4(3)
O(11)-Gd(5)-O(30)	121.9(2)
O(7)-Gd(5)-O(30)	136.7(2)
O(1)-Gd(5)-O(30)	125.3(2)
O(41)-Gd(5)-O(30)	67.9(2)
O(42)-Gd(5)-O(30)	75.9(2)
O(29)-Gd(5)-O(30)	50.4(2)
O(40)-Gd(5)-O(30)	66.7(3)
Gd(2)-O(25)-Gd(1)	109.02(19)
Gd(2)-O(25)-Gd(3)	108.70(19)
Gd(1)-O(25)-Gd(3)	108.79(19)
Gd(2)-O(25)-H(25)	106(6)

Table S3. Selected bond lengths [Å] and angles [°] for compound **2**.

Co(1)-O(11)	1.925(12)
Co(1)-O(1)	1.929(13)
Co(1)-O(7)	1.933(13)
Co(1)-O(33)	1.978(12)
Gd(1)-O(18)	2.280(11)
Gd(1)-O(3)	2.319(11)
Gd(1)-O(21)	2.320(12)
Gd(1)-O(32)	2.387(12)
Gd(1)-O(31)	2.393(14)
Gd(1)-O(9)	2.405(12)
Gd(1)-O(25)	2.465(12)
Gd(1)-Gd(3)	3.9035(15)
Gd(2)-O(2)	2.289(13)
Gd(2)-O(13)	2.314(12)

Gd(2)-O(30)	2.320(14)
Gd(2)-O(6)	2.328(12)
Gd(2)-O(22)	2.329(12)
Gd(2)-O(25)	2.400(11)
Gd(2)-O(5)	2.633(12)
Gd(2)-Gd(3)	3.8876(15)
Gd(3)-O(14)	2.264(13)
Gd(3)-O(17)	2.311(12)
Gd(3)-O(5)	2.313(11)
Gd(3)-O(29)	2.338(13)
Gd(3)-O(10)	2.349(13)
Gd(3)-O(25)	2.373(11)
Gd(3)-O(9)	2.516(12)
Gd(4)-O(23)	2.213(14)

Gd(4)-O(15)	2.266(13)
Gd(4)-O(19)	2.279(12)
Gd(4)-O(28)	2.30(2)
Gd(4)-O(26)	2.41(3)
Gd(4)-O(27)	2.59(2)
O(1)-P(1)	1.511(13)
O(2)-P(1)	1.510(13)
O(3)-P(1)	1.519(14)
O(4)-P(1)	1.635(13)
O(5)-P(2)	1.527(12)
O(6)-P(2)	1.517(12)
O(7)-P(2)	1.500(13)
O(8)-P(2)	1.617(13)
O(9)-P(3)	1.483(12)
O(10)-P(3)	1.518(14)
O(11)-P(3)	1.529(13)
O(12)-P(3)	1.600(12)
O(13)-P(4)	1.534(14)
O(14)-P(4)	1.519(14)
O(15)-P(4)	1.481(13)
O(16)-P(4)	1.611(15)
O(17)-P(5)	1.494(13)
O(18)-P(5)	1.496(13)
O(19)-P(5)	1.519(13)
O(20)-P(5)	1.616(14)
O(21)-P(6)	1.489(12)
O(22)-P(6)	1.504(13)
O(23)-P(6)	1.520(14)
O(24)-P(6)	1.612(14)
O(11)-Co(1)-O(1)	114.9(6)
O(11)-Co(1)-O(7)	109.7(6)
O(1)-Co(1)-O(7)	119.0(5)
O(11)-Co(1)-O(33)	105.0(5)
O(1)-Co(1)-O(33)	104.9(5)
O(7)-Co(1)-O(33)	101.2(5)
O(18)-Gd(1)-O(3)	170.1(4)
O(18)-Gd(1)-O(21)	90.1(4)
O(3)-Gd(1)-O(21)	94.5(4)
O(18)-Gd(1)-O(32)	88.1(5)
O(3)-Gd(1)-O(32)	84.7(5)
O(21)-Gd(1)-O(32)	74.4(4)

O(18)-Gd(1)-O(31)	82.6(4)
O(3)-Gd(1)-O(31)	88.5(5)
O(21)-Gd(1)-O(31)	144.1(4)
O(32)-Gd(1)-O(31)	70.3(5)
O(18)-Gd(1)-O(9)	95.0(4)
O(3)-Gd(1)-O(9)	86.5(4)
O(21)-Gd(1)-O(9)	143.3(4)
O(32)-Gd(1)-O(9)	141.9(4)
O(31)-Gd(1)-O(9)	72.5(4)
O(18)-Gd(1)-O(25)	76.5(4)
O(3)-Gd(1)-O(25)	113.1(4)
O(21)-Gd(1)-O(25)	76.1(4)
O(32)-Gd(1)-O(25)	146.5(4)
O(31)-Gd(1)-O(25)	134.8(4)
O(9)-Gd(1)-O(25)	70.0(4)
O(2)-Gd(2)-O(13)	162.1(5)
O(2)-Gd(2)-O(30)	107.4(5)
O(13)-Gd(2)-O(30)	90.0(5)
O(2)-Gd(2)-O(6)	87.7(5)
O(13)-Gd(2)-O(6)	100.7(5)
O(30)-Gd(2)-O(6)	76.9(5)
O(2)-Gd(2)-O(22)	88.3(5)
O(13)-Gd(2)-O(22)	91.2(5)
O(30)-Gd(2)-O(22)	78.1(5)
O(6)-Gd(2)-O(22)	152.2(4)
O(2)-Gd(2)-O(25)	78.7(4)
O(13)-Gd(2)-O(25)	83.6(4)
O(30)-Gd(2)-O(25)	156.6(5)
O(6)-Gd(2)-O(25)	126.3(4)
O(22)-Gd(2)-O(25)	79.6(4)
O(2)-Gd(2)-O(5)	88.1(4)
O(13)-Gd(2)-O(5)	83.0(4)
O(30)-Gd(2)-O(5)	132.4(5)
O(6)-Gd(2)-O(5)	58.5(4)
O(22)-Gd(2)-O(5)	148.7(4)
O(25)-Gd(2)-O(5)	69.2(4)
O(14)-Gd(3)-O(17)	89.1(5)
O(14)-Gd(3)-O(5)	84.0(5)
O(17)-Gd(3)-O(5)	156.6(4)
O(14)-Gd(3)-O(29)	74.9(5)
O(17)-Gd(3)-O(29)	92.8(5)

O(5)-Gd(3)-O(29)	106.8(5)
O(14)-Gd(3)-O(10)	148.8(5)
O(17)-Gd(3)-O(10)	109.8(4)
O(5)-Gd(3)-O(10)	86.7(4)
O(29)-Gd(3)-O(10)	79.5(5)
O(14)-Gd(3)-O(25)	80.0(5)
O(17)-Gd(3)-O(25)	81.4(4)
O(5)-Gd(3)-O(25)	75.4(4)
O(29)-Gd(3)-O(25)	154.4(5)
O(10)-Gd(3)-O(25)	126.0(4)
O(14)-Gd(3)-O(9)	149.6(4)
O(17)-Gd(3)-O(9)	88.2(4)
O(5)-Gd(3)-O(9)	86.5(4)
O(29)-Gd(3)-O(9)	135.5(4)
O(10)-Gd(3)-O(9)	58.6(4)
O(25)-Gd(3)-O(9)	69.6(4)
O(23)-Gd(4)-O(15)	88.7(5)
O(23)-Gd(4)-O(19)	88.0(5)

O(15)-Gd(4)-O(19)	93.2(5)
O(23)-Gd(4)-O(28)	172.9(8)
O(15)-Gd(4)-O(28)	85.3(8)
O(19)-Gd(4)-O(28)	88.6(6)
O(23)-Gd(4)-O(26)	89.8(7)
O(15)-Gd(4)-O(26)	79.2(7)
O(19)-Gd(4)-O(26)	172.1(7)
O(28)-Gd(4)-O(26)	92.8(9)
O(23)-Gd(4)-O(27)	94.3(8)
O(15)-Gd(4)-O(27)	163.3(7)
O(19)-Gd(4)-O(27)	103.3(7)
O(28)-Gd(4)-O(27)	92.5(10)
O(26)-Gd(4)-O(27)	84.4(8)
Gd(3)-O(5)-Gd(2)	103.4(5)
Gd(1)-O(9)-Gd(3)	105.0(4)
Gd(3)-O(25)-Gd(2)	109.1(4)
Gd(3)-O(25)-Gd(1)	107.5(4)
Gd(2)-O(25)-Gd(1)	116.6(5)

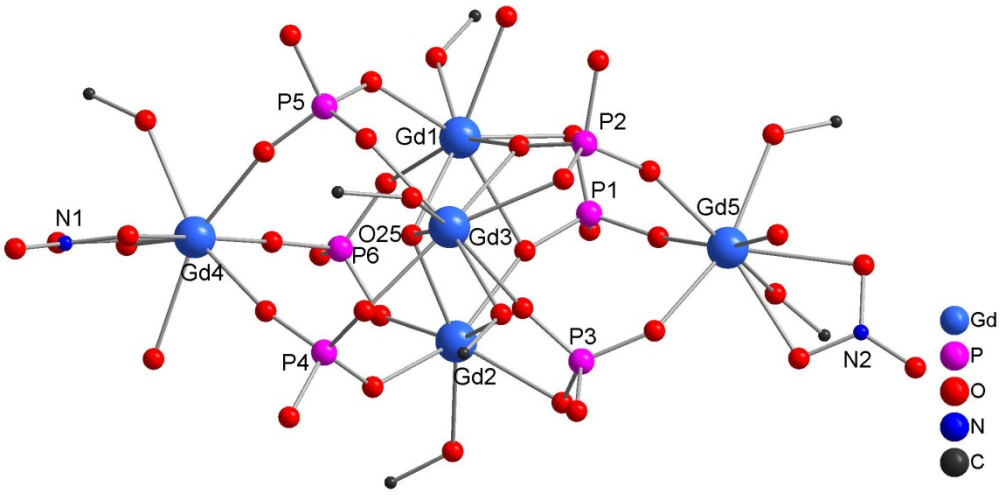

Figure S5. Core structure of compound $[Gd_5(\mu_3\text{-}OH)(NO_3)_2(dipp)_6(CH_3OH)_7(H_2O)_4].5CH_3OH$ (**1**).

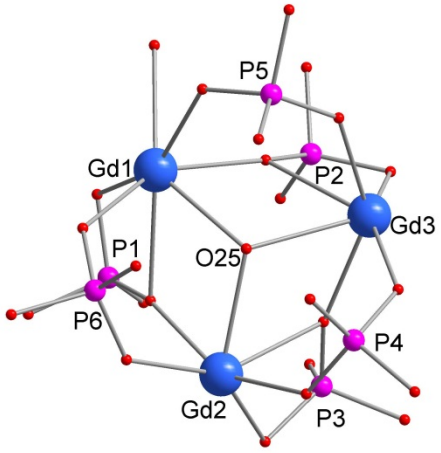

Figure S6. View of the $[Gd(\mu_3\text{-}OH)(dipp)_6]$ triangle in **1**.

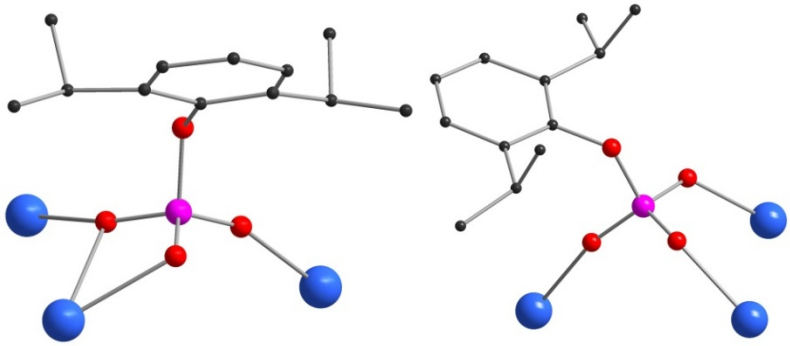

Figure S7. [3.211] and [3.111] Binding modes of phosphate ligand.

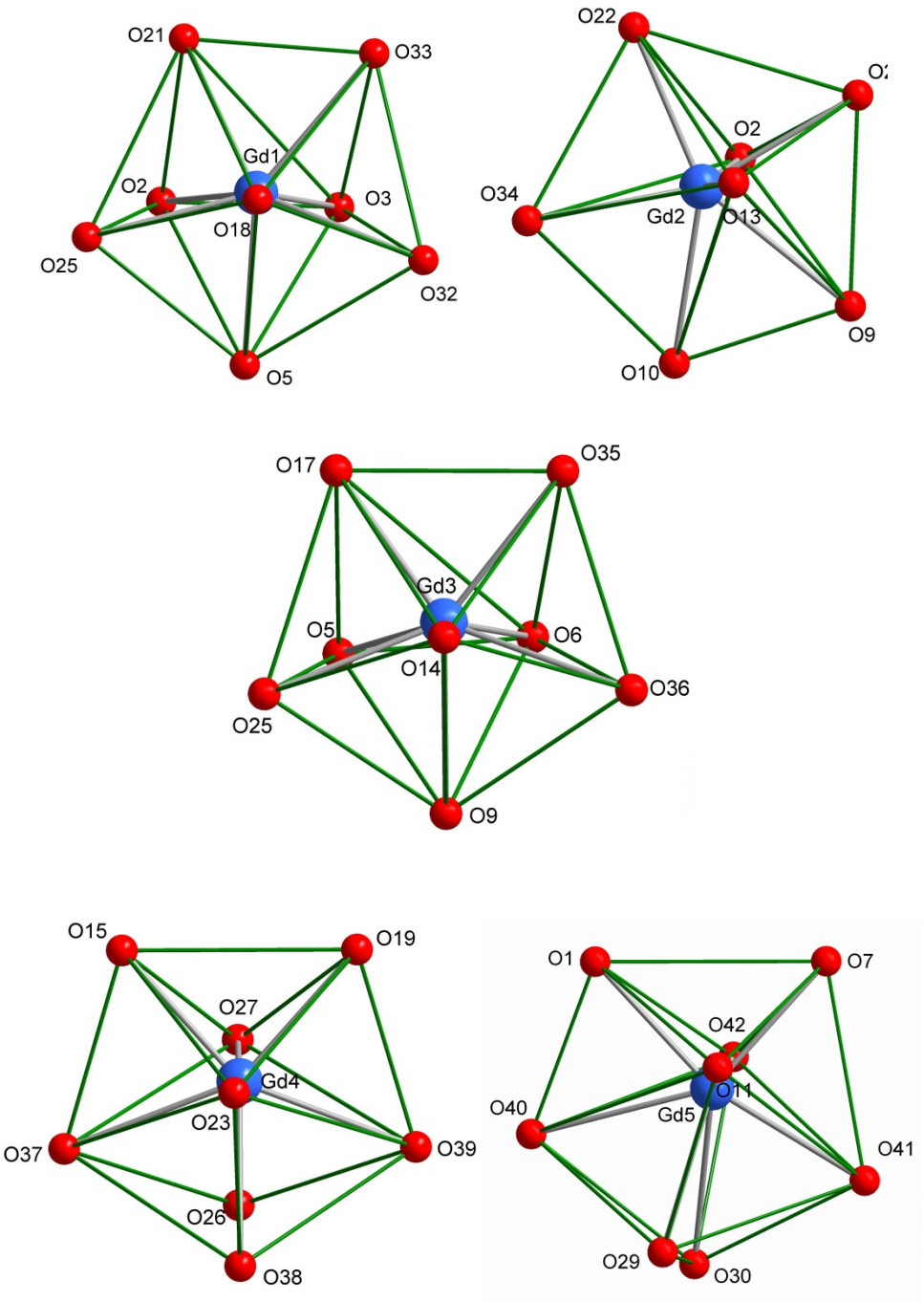

Figure S8. Coordination environment of Gd(III) ions in compound **1**.

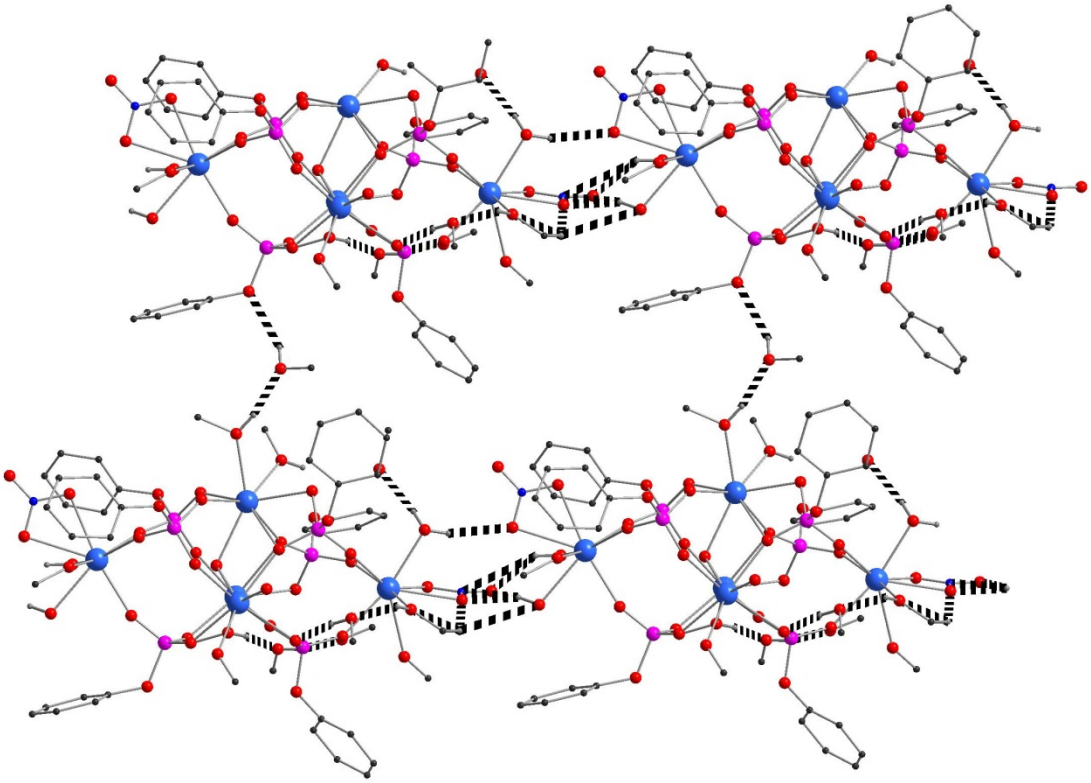

Figure S9. Intramolecular and intermolecular H-bonding in **1** leading to the formation of supramolecular 2D sheets of pentanuclear cluster.

Table S4. Hydrogen bonds for compound **1** [Å and °].

D-H...A	d(D-H)	d(H...A)	d(D...A)	<(DHA)
O(32)-H(32A)...O(45)#1	0.88	2.52	3.160(13)	130.4
O(37)-H(37B)...O(31)#2	0.89	2.09	2.773(11)	133.0
O(38)-H(38B)...O(30)#2	0.87	2.02	2.802(9)	148.4
O(38)-H(38B)...O(31)#2	0.87	2.51	3.287(11)	149.1
O(41)-H(41A)...O(26)#1	0.88	2.31	3.053(9)	141.9
O(41)-H(41B)...O(47)	0.88	1.92	2.615(10)	134.8
O(43)-H(43A)...O(44)	0.84	1.90	2.68(2)	154.3
O(45)-H(45)...O(3)#2	0.84	1.84	2.661(10)	165.8
O(46)-H(46A)...O(24)	0.84	2.25	2.968(9)	143.5
O(34)-H(34)...O(43)	0.876(10)	1.807(15)	2.674(9)	170(3)
O(35)-H(35)...O(46)#3	0.875(10)	1.863(17)	2.723(9)	167(4)
O(36)-H(36)...O(12)	0.876(10)	2.28(9)	2.913(8)	129(9)
O(42)-H(42)...O(45)#1	0.875(10)	1.91(7)	2.704(12)	150(12)
O(25)-H(25)...O(15)	0.86(9)	2.49(9)	3.221(7)	143(8)

Symmetry transformations used to generate equivalent atoms:
#1 x,y-1,z #2 x,y+1,z #3 x+1,y,z

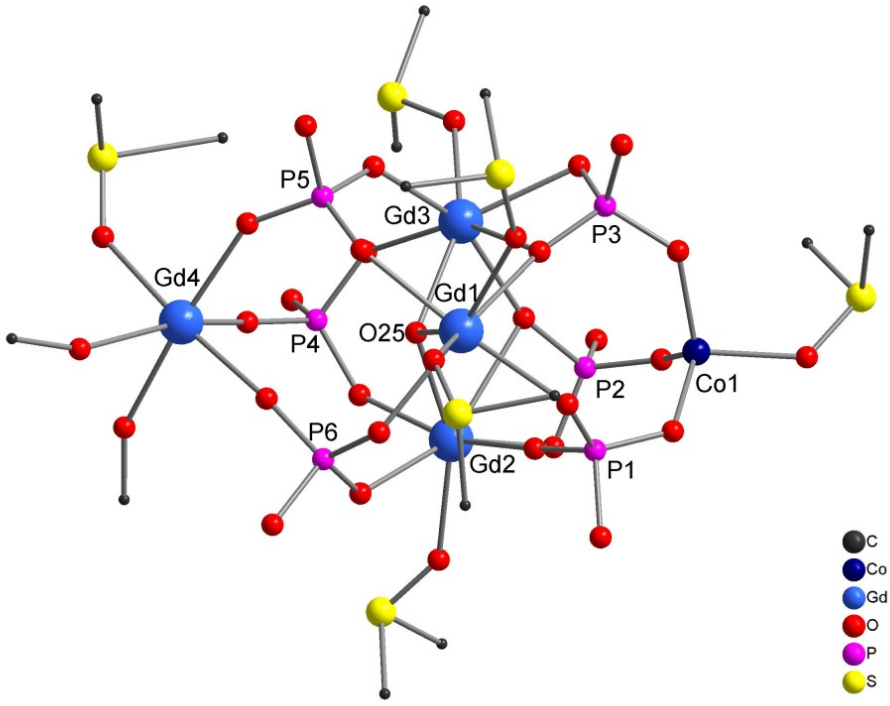

Figure S10. Core structure of

$[Gd_4Co_1(\mu_3\text{-}O)(dipp)_6(DMSO)_6(MeOH)_2].H_2O$ **(2)**.

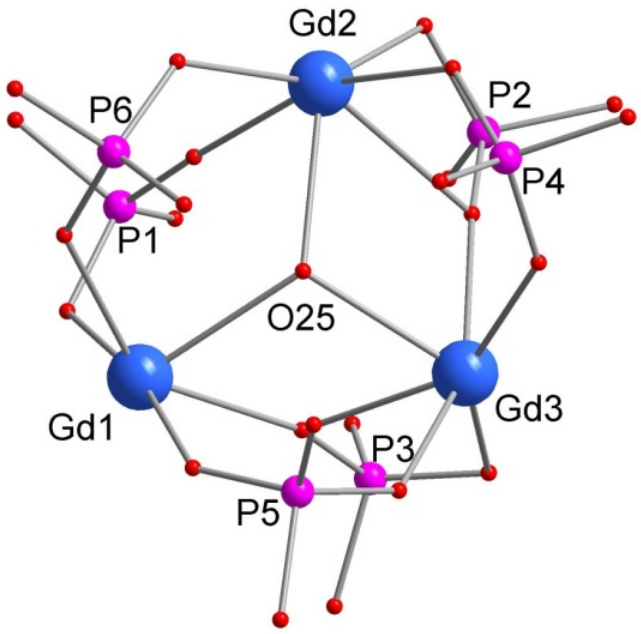

Figure S11. View of the $[Gd_3(\mu_3\text{-}O)(dipp)_6]$ triangle in compound **2.**

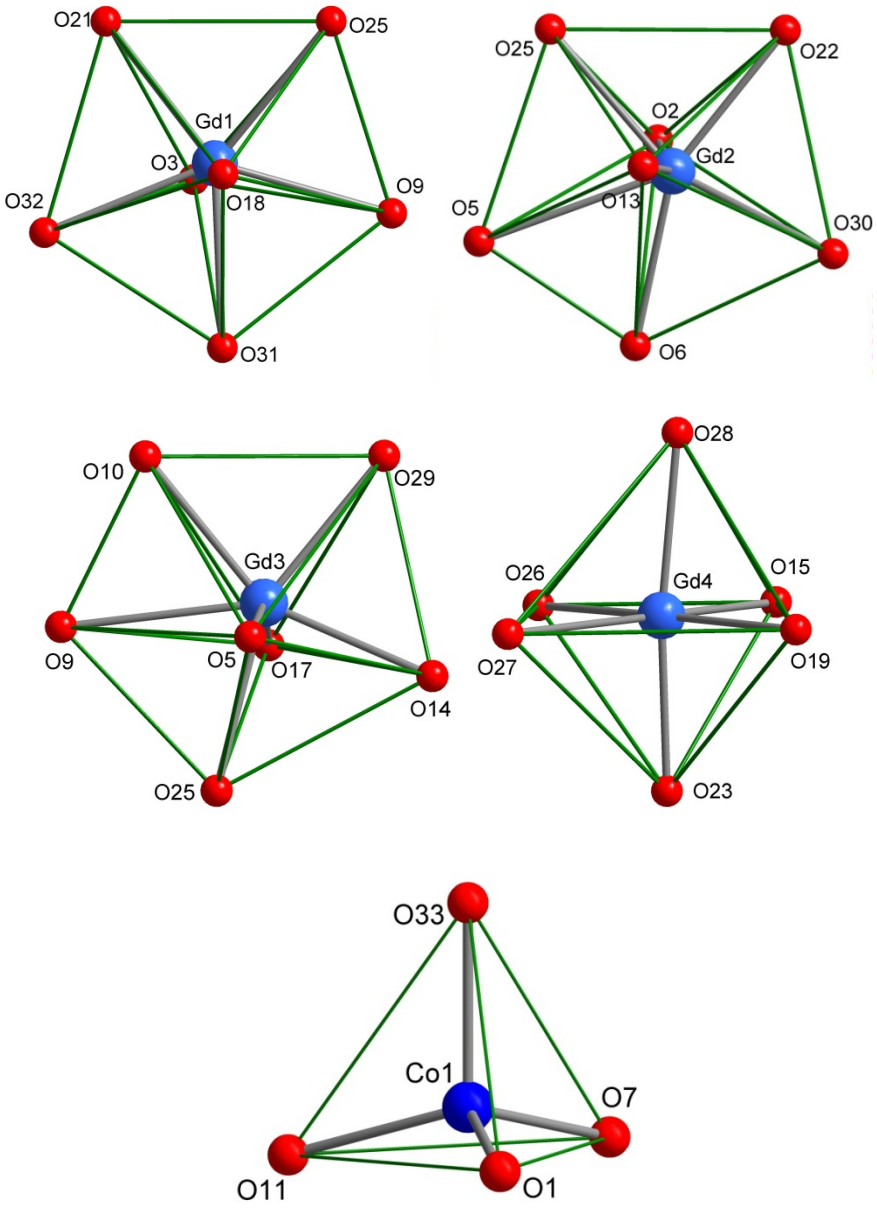

Figure S12. Coordination environment of the metal ions in compound **2**.

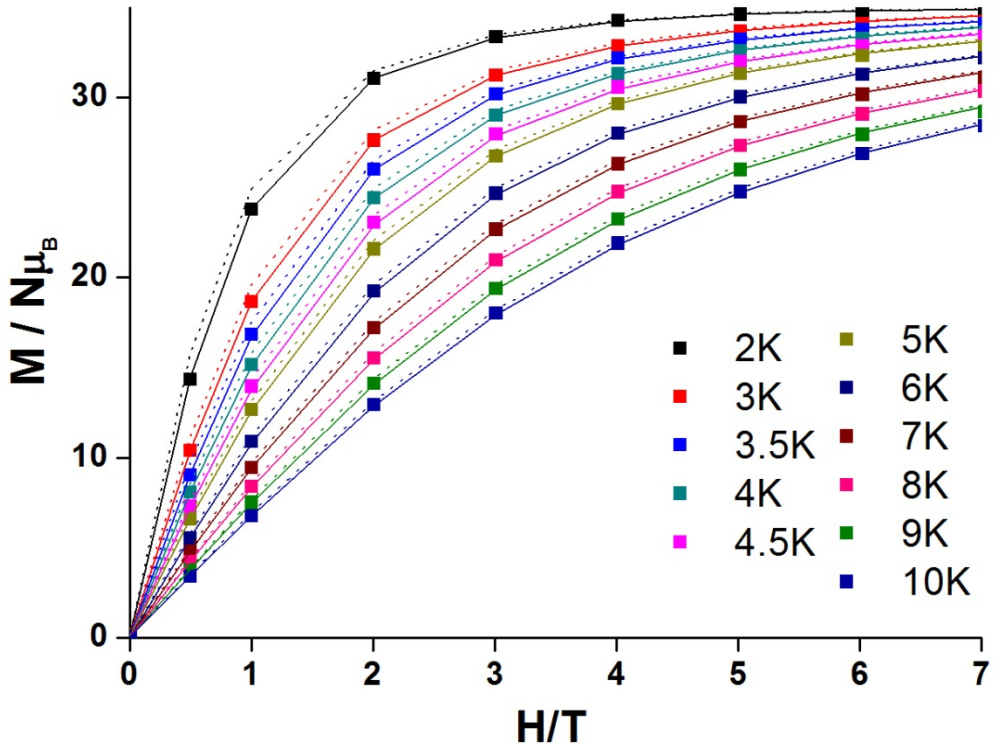

Figure S13. Field dependence of magnetization for compound **1**.

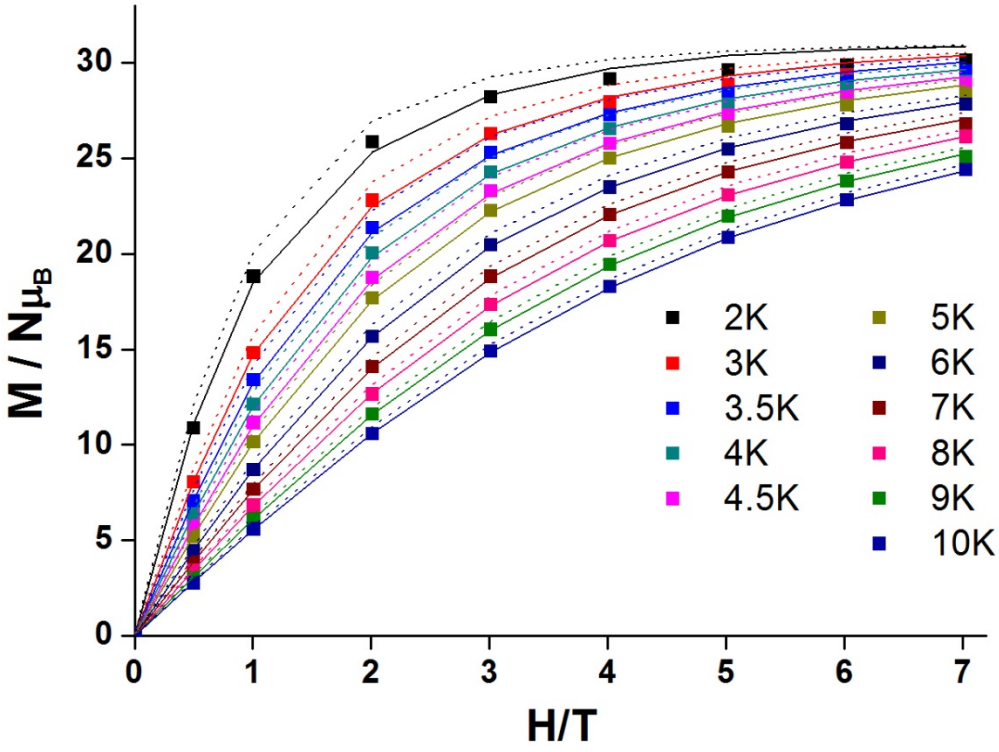

Figure S14. Field dependence of magnetization for compound **2**.

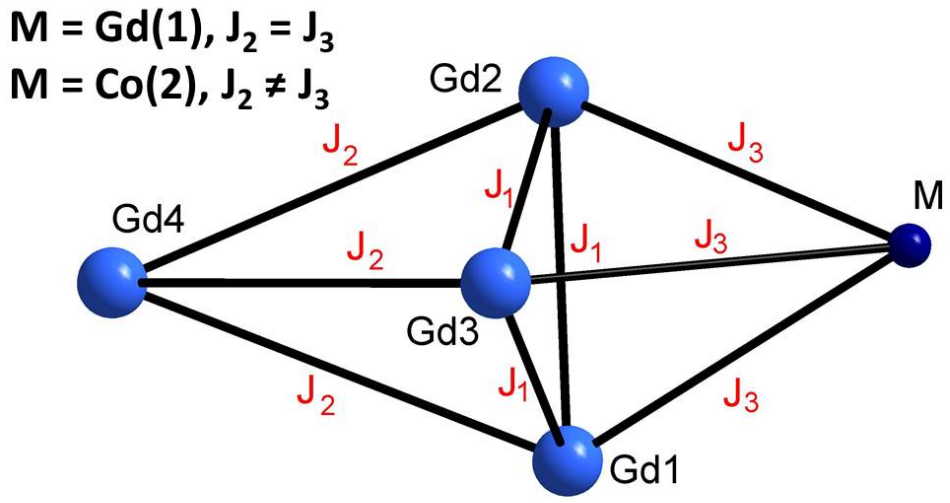

Figure S15. Exchange interaction between the metal ions in **1** and **2**

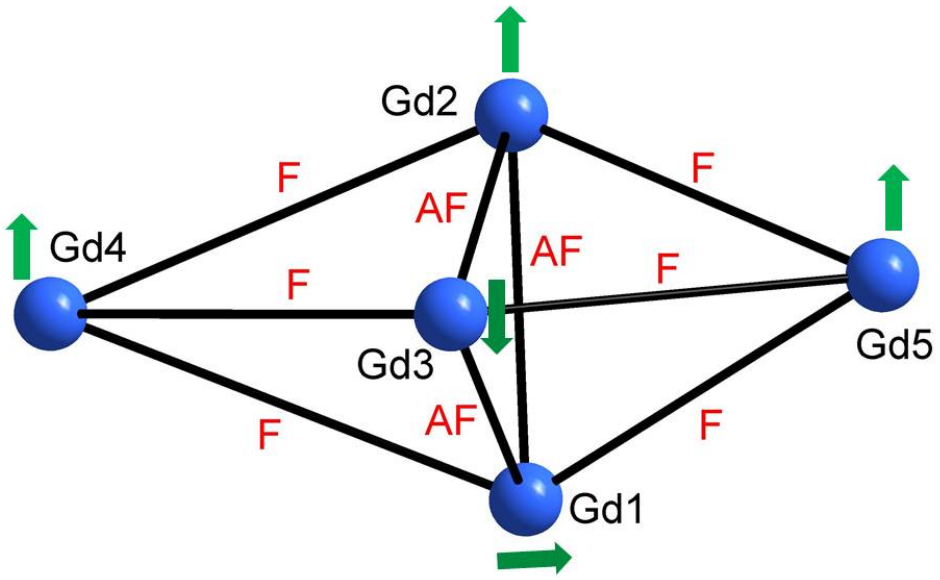

Figure S16. Depiction of the indicated exchange interaction between the metal ions and resulting spin frustration.

Computational details:

The broken symmetry method[7] has been employed to evaluate *J* constants in complexes **1** and **2**, as it is found to estimate exchange values in variety of complexes.[8] We have performed all our calculations using Gaussian 09[9] suite of programs. A hybrid B3LYP[10] functional along with Cundari-Stevens (CS) relativistic effective core potential on the Gd atom[11], TZV quality basis set on Ni, Co, Fe, Mn, Cu atoms[12] and TZVP quality basis set on S atom with SVP basis set[13] for the rest of the atoms were employed to evaluate exchange constants.

For the $\{Gd^{III}_5\}$ complex, the following exchange Hamiltonian has been used,

$$\hat{H}_{Ex} = -J_1(S_{Gd1}.S_{Gd2} + S_{Gd2}.S_{Gd3} + S_{Gd1}.S_{Gd3}) - J_2(S_{Gd1}.S_{G} \quad (1)$$

For the $\{Gd^{III}_4Co^{II}\}$ complex, the following exchange Hamiltonian has been used,

$$\hat{H}_{Ex} = -J_1(S_{Gd1}.S_{Gd2} + S_{Gd2}.S_{Gd3} + S_{Gd1}.S_{Gd3}) - J_2(S_{Gd1}.S_{G} - J_3(S_{Gd1}.S_{Co5} + S_{Gd2}.S_{Co5} + S_{Gd3}.S_{Co5}) \quad (2)$$

For the dinuclear model $\{Gd^{III}_4 3d^{II}\}$ complexes [3d= Cu, Fe, Mn, Ni], the following exchange Hamiltonian has been used,

$$\hat{H}_{Ex} = -J(S_{Gd}.S_{3d}) \quad (3)$$

The exchange interaction values (J_1 and J_2) in complex **1** is evaluated form three different spin configurations- (a) High spin configuration (b) spin on $Gd_{(3)}$ (down) (c) spin on $Gd_{(4)}$ (down) and in the case of complex 2, four different configuration have been employed- (a) High spin configuration (b) spin on $Gd_{(2)}$ (down) (c) spin on $Gd_{(4)}$ (down) (c) spin on $Co_{(5)}$ (down).

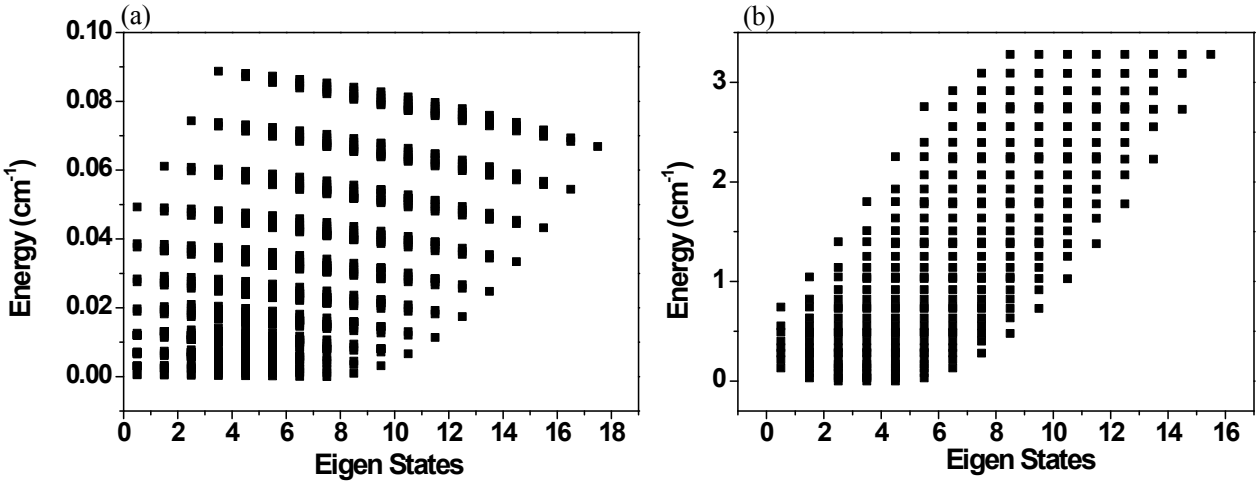

Figure S17. Eigen value plots for complexes **1** (a) and **2** (b) using DFT *J* values

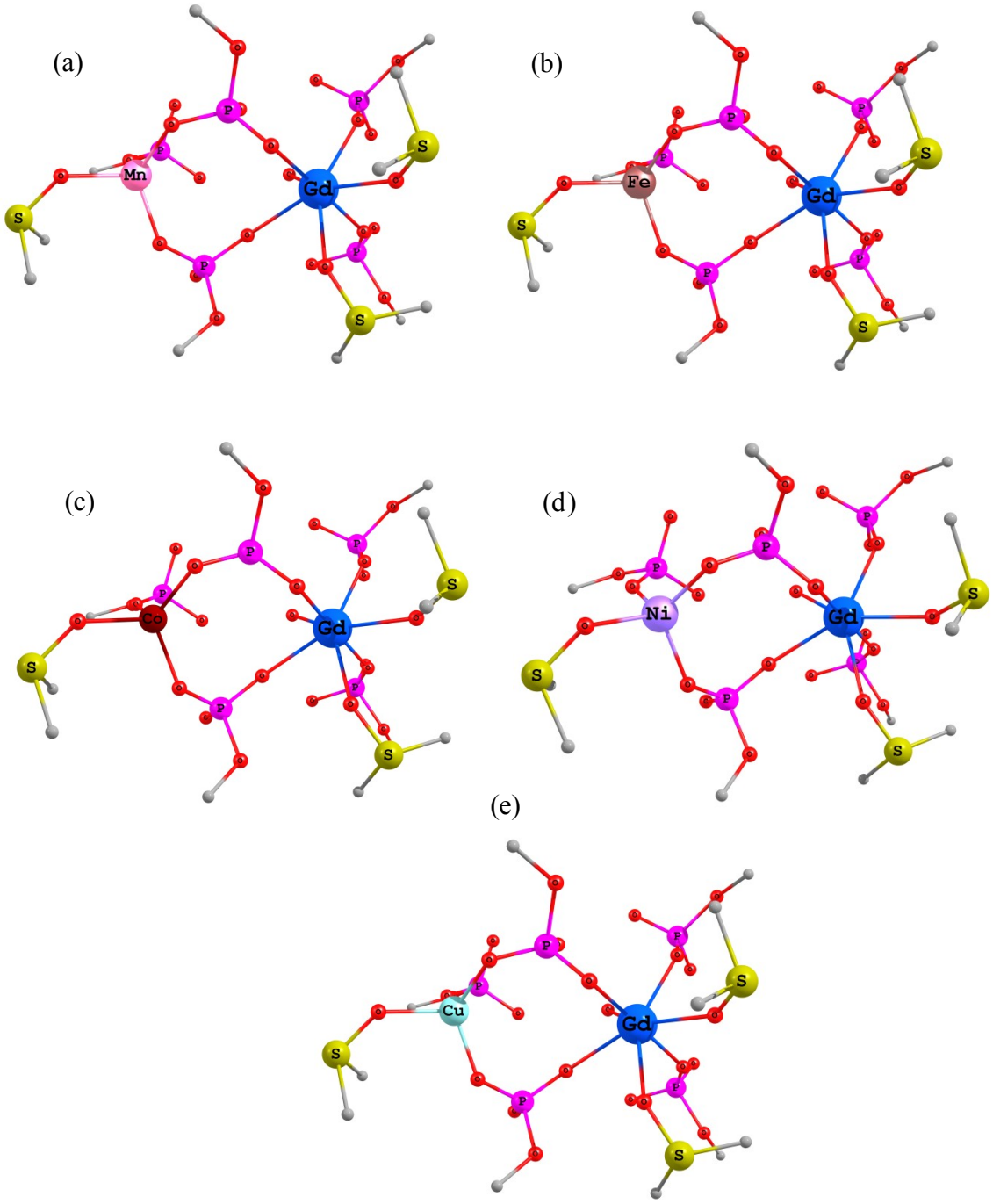

Figure S18. Model complexes employed for extracting *J* values in first row transition metal ions.

References:

1. G. M.Kosolapoff, C. K. Arpke, R. W. Lamb and H. Reich, *J. Chem. Soc., Sect. C: Organic* 1968, **7**, 815.
2. A. C. Kalita, N. Gogoi, R. Jangir, S. Kuppuswamy, M. G. Walawalkar and R. Murugavel, *Inorg. Chem.*, 2014, **53**, 8959.
3. L. J. Farrugia, WinGX, Version 1.64.05; *J. Appl. Crystallogr*. 1999, **32**, 837.

4. A. Altomare, G. Cascarano, C. Giacovazzo and A. Gualardi, *J. Appl. Crystallogr.* 1993, **26**, 343.
5. G. M. Sheldrick, *Acta Cryst*., 2008, **A64**, 112.
6. A. L. Spek, *J. Appl. Crystallogr*., 2003, **36**, 7.
7. L. Noodleman, *J. Chem. Phys*., 1981, **74**, 5737.
8. (a) E. Ruiz, S. Alvarez, J. Cano and P. Alemany, *J. Comput. Chem*., 1999, **20**, 1391; (b) E. Ruiz, A. Rodriguez-Fortea, J. Cano, S. Alvarez and P. Alemany, *J. Comput. Chem*., 2003, **24**, 982; (c) G. Rajaraman, J. Cano, E. K. Brechin and E. J. L. McInnes, *Chem. Commun.*, 2004, 1476; (d) P. Christian, G. Rajaraman, A. Harrison, J. J. W. McDouall, J. Raftery and R. E. P. Winpenny, *Dalton Trans*., 2004, 2550; (e) G. Rajaraman, M. Murugesu, E. C. Sanudo, M. Soler, W. Wernsdorfer, M. Helliwell, C. Muryn, J. Raftery, S. J. Teat, G. Christou and E. K. Brechin, J. Am. Chem. Soc., 2004, **126**, 15445; (f) S. Sasmal, S. Hazra, P. Kundu, S. Dutta, G. Rajaraman, E. C. Sanudo and S. Mohanta, Inorg. Chem., 2011, **50**, 7257.
9. M. J. Frisch, G. W. Trucks, H. B. Schlegel, G. E. Scuseria, M. A. Robb, J. R. Cheeseman, G. Scalmani, V. Barone, B. Mennucci, G. A. Petersson, H. Nakatsuji, M. Caricato, X. Li, H. P. Hratchian, A. F. Izmaylov, J. Bloino, G. Zheng, J. L. Sonnenberg, M. Hada, M. Ehara, K. Toyota, R. Fukuda, J. Hasegawa, M. Ishida, T. Nakajima, Y. Honda, O. Kitao, H. Nakai, T. Vreven, J. A. Montgomery Jr., J. E. Peralta, F. Ogliaro, M. Bearpark, J. J. Heyd, E. Brothers, K. N. Kudin, V. N. Staroverov, R. Kobayashi, J. Normand, K. Raghavachari, A. Rendell, J. C. Burant, S. S. Iyengar, J. Tomasi, M. Cossi, N. Rega, J. M. Millam, M. Klene, J. E. Knox, J. B. Cross, V. Bakken, C. Adamo, J. Jaramillo, R. Gomperts, R. E. Stratmann, O. Yazyev, A. J. Austin, R. Cammi, C. Pomelli, J. W. Ochterski, R. L. Martin, K. Morokuma, V. G. Zakrzewski, G. A. Voth, P. Salvador, J. J. Dannenberg, S. Dapprich, A. D. Daniels, O. Farkas, J. B. Foresman, J. V. Ortiz, J. Cioslowski and D. J. Fox, GAUSSIAN 09 (Revision A.02), Gaussian, Inc., Wallingford, CT, 2009
10. A. D. Becke, *J. Chem. Phys*., 1993, **98**, 5648.
11. T.R. Cundari, W.J. Stevens, *J. Chem. Phys*. 1993, **98**, 5555
12. A. Schafer, H. Horn and R. Ahlrichs, *J. Chem. Phys*., 1992, 97.
13. A. Schafer, C. Huber, R. Ahlrichs, *J. Chem. Phys*. 1994, **100**, 5829.